Journal of Aerosol Science 131 (2019) 41–47

Contents lists available at ScienceDirect

Journal of Aerosol Science

journal homepage: www.elsevier.com/locate/jaerosci

The role of blank filter mass in attenuation measurements using an off-line transmissometer

V. Sreekanth[a,*], Cathryn Tonne[b], Maëlle Salmon[b], S. Arulselvan[c], Julian D. Marshall[a]

[a] Department of Civil and Environmental Engineering, University of Washington, Seattle, WA, United States
[b] ISGlobal, Universitat Pompeu Fabra, CIBER Epidemiología y Salud Pública, Barcelona, Spain
[c] Department of Environmental Health Engineering, Sri Ramachandra University, Chennai, Tamil Nadu, India

ARTICLE INFO

Keywords:
Emfab
Filter thickness
Transmittance
Light attenuation

ABSTRACT

We describe how reference filter characteristics (unexposed weights) can influence instrument-reported attenuation (thereby black carbon concentrations) using the OT21 (SootScan Optical Transmissometer), in the case of Emfab filters. Reference filters (unexposed filters) with higher unexposed weights (pre-weights) compared to that of sample filters are found to reduce the instrument-reported aerosol sample attenuation measurement; reference filters weighing less than the sample filter results in the reverse outcome. This sensitivity can lead to significant under- and over-estimation by the instrument (estimated mean absolute error: ~ 10 and 16 ATN units for infrared (IR) and ultraviolet (UV) channels, respectively, in our tests, which represent 44% and 15% errors, respectively). We find that the error is linear with respect to difference in the unexposed filter weights of the sample and reference filters. We report two equations (one for IR, one for UV) for correcting the Transmissometer output based on experimental data, which allow use of any unexposed Emfab filter as the reference filter; application of correction parameters to data here reduces the error to 2 and 3 ATN units, respectively, for IR and UV (10% and 3% errors, respectively).

1. Introduction

Black carbon (BC) aerosols are relevant to the global climate and to human health. BC impacts climate by attenuating solar radiation, influencing cloud processes, and altering the melt rate of snow and ice cover (Bond et al., 2013). Exposure to BC is associated with adverse health impacts such as higher blood pressures (Baumgartner et al., 2014) and cardiovascular risk (Ostro et al., 2008) and is associated with health outcomes independent of particulate matter (Janssen et al., 2011). On the other hand, ultraviolet absorbing particulate matter (UVPM), mainly emitted by wood and biomass burning activities can significantly affect tropospheric photochemistry and interact/absorb solar radiation (Kirchstetter & Thatcher, 2012).

Several techniques are available for estimating BC and UVPM mass concentrations based on optical, thermal and acoustic principles. Multiple authors have compared results from various instruments and methods using these principles (Ahmed et al., 2009; Davy, Tremper, Nicolosi, Quincey, & Fuller, 2017; Presler-Jur, Doraiswamy, Hammond, & Rice, 2017; Ram, Sarin, & Tripathi, 2010). Reflectometry (Delumyea, Lih-Ching, & Macias, 1980) and transmissometry (Dutkiewicz et al., 2014; Hill, 1936; Moosmüller, Chakrabarty, & Arnott, 2009) are well established optical techniques for estimating the darkness of a sample collected on a substrate, in which darkness is proportional to BC concentration (Beer-Lambert Law).

* Corresponding author.
E-mail address: sree_hcu@yahoo.co.in (V. Sreekanth).

https://doi.org/10.1016/j.jaerosci.2019.03.001
Received 5 October 2018; Received in revised form 31 January 2019; Accepted 2 March 2019
Available online 06 March 2019
0021-8502/

Transmissometry (e.g. Dutkiewicz et al., 2014) involves filter-based sampling of aerosol particles (air is drawn through a filter; particles deposit onto the filter) followed by measurement in the transmissometer of the blackness of the exposed filter relative to a reference (i.e., unexposed) filter. Optical attenuation is measured by transmitting a monochromatic light signal through these filter papers and measuring the subsequent spectral attenuation.

We report sensitivity of transmissometer measurements to a reference filter (Emfab), which to our knowledge has not been previously described in the literature. In a recent study, Presler-Jur et al. (2017) reported large variations in the attenuation of the Teflon filter blanks within filter lots. We investigated whether this sensitivity is related to filter unexposed weight. Finally, we propose, implement, and test an approach for generating a correction equation to address the impact of variation in reference filter unexposed weight. This short communication contributes to the peer-reviewed literature by providing correction factors for transmissometer measurements.

2. Material and methods

Analysis and results presented here are part of the Cardiovascular Health effects of Air pollution in Telangana, India (CHAI) project (http://www.chaiproject.org). Details regarding the aims, objectives and filter sampling protocols are given elsewhere (Tonne et al., 2017).

We used an offline SootScan Optical Transmissometer (Model: OT21, Magee Scientific, Berkeley, California, USA). The

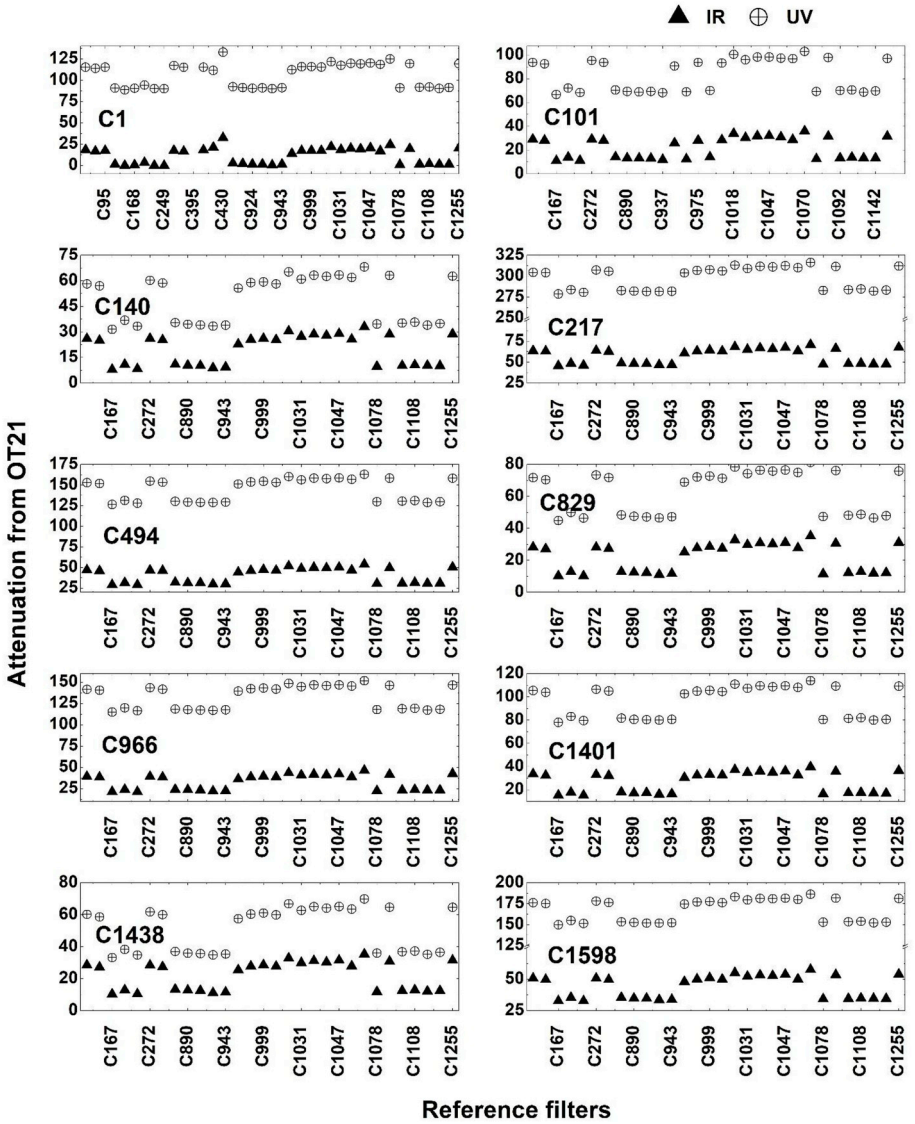

Fig. 1. IR and UV attenuation values for ten randomly drawn samples (C1, C101, C140, C217, C494, C829, C966, C1401, C1438, C1598) measured against various reference filters. X-axis labels correspond to reference filter label.

Transmissometer measures optical attenuation of an aerosol-loaded filter (the sample) relative to a reference (i.e., unexposed) filter at two wavelengths, infrared (880 nm) and ultraviolet (370 nm). We operated the instrument in accordance with manufacturer's protocol (mageesci.com/EACworkshop2016/MANUALS/OT21/OT21_UsersManual_V52.pdf). The instrument accepts three filter sizes (25 mm, 37 mm and 47 mm diameter). A variety of filter media types (e.g., Quartz fiber, Teflon coated borosilicate glass fiber, Teflon membrane filters) may be used. The sensitivity of the instrument is 1 ATN unit and the optimal maximum loading is 125 ATN units (above which the linearity of the instrument is impaired). Operating the instrument involves inserting two filters (the sample filter; the reference filter); the instrument output is optical attenuation (ATN; unitless; defined as the gradual reduction in the intensity of the optical signal while propagating through the material medium) at each of the two wavelengths (λ). ATN is calculated as

$$ATN = 100^* \ln (I_o/I), \quad (1)$$

where, I_o and I are the light transmission of the blank reference and sample filters, respectively. Importantly, this equation assumes that transmission for the reference filter would be equal to the transmission for the sample if the sample had no light attenuating material on the filter.

The CHAI project collected ~1700 measurements of 24-h $PM_{2.5}$ for personal and ambient monitoring. SKC pumps (Model: 224-PCMTX8, SKC Ltd, Dorset, UK) drew air through a cyclone separator (cut-point: 2.5 μm) attached to a cassette containing 37-mm filter papers. Pallflex Emfab filter media were used for all samples. Emfab filters are pure borosilicate glass microfibers, reinforced with woven glass cloth and bonded with Polytetrafluoroethylene (PTFE). These filters are characterised with low air resistance and low moisture pickup and high durability, making them well–suited for gravimetric mass measurements. The filter weighing protocol can be found in Balakrishnan et al. (2015). Transmissometer measurements were conducted on all filters. Reference filters were from the same lot and batch as the that of sample filters. Precisely, no reference filters from lots/batches other than the ones utilized for the project are used for the measurements. We defined the lots using the lot numbers printed on each box. By 'batch' we mean the box containing 100 filters. CHAI project used more than 2000 filters (including pilot study and main study), all the filters are not from the same lots. We used filters from more than two lots and several batches.

We assessed the Transmissometer measurements by measuring ten exposed sample filters with each of 30 reference filters (i.e., 300 measurements in total). We then used regression analysis (R-Core Team, 2016) to explore the relationship between attenuation and the difference in the unexposed weight of the sample filter and that of the reference filter. Analysis of these data (below) uncovered the sensitivity and also suggested the correction equation approach described below. The suggested approach has been tested by calculating the mean absolute error in the attenuation values (for both IR and UV channels) before and after the correction.

Linear regression models constructed in the study are compared using the Akaike's Criterion (AIC).

3. Results and discussion

The IR and UV attenuations for ten sample filters (C1, C101, C140, C217, C494, C829, C966, C1401, C1438, C1598) compared to different reference filters are shown in Fig. 1. For sample C1, for example, instrument-reported attenuation varied between 0.1 and 32 ATN (IR) and between 80 and 133 ATN (UV). Thus, Fig. 1 demonstrates that the Transmissometer reading for a single sample filter can vary by reference filter. The coefficient of variation (COV) for the ten sample attenuation values ranged between 0.16 (0.05) and 0.80 (0.28) for IR (UV); the median COV among the ten samples is 0.37 (0.14) for IR (UV). Similarly, for all other filters, the Transmissometer attenuation value was not constant for IR and for UV. We investigated whether variability in the attenuation was explained by differences in filter unexposed weights.

The distribution of the unexposed weights of all Emfab 37 mm filters is shown in Fig. 2. The unexposed filter weights varied between 47.5 and 59.5 mg and the distribution appeared to be bimodal. To understand the impact of filter weights on

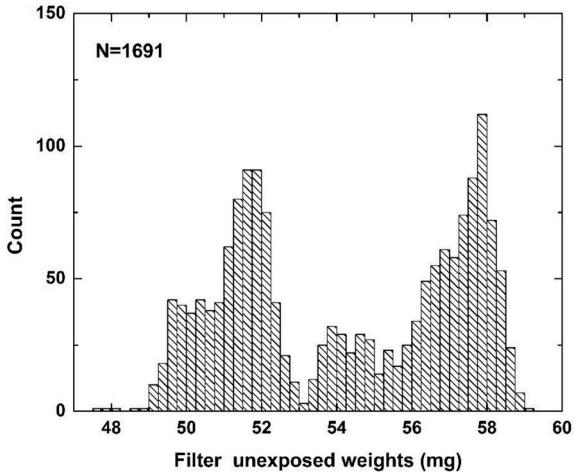

Fig. 2. Distribution of unexposed filter weights.

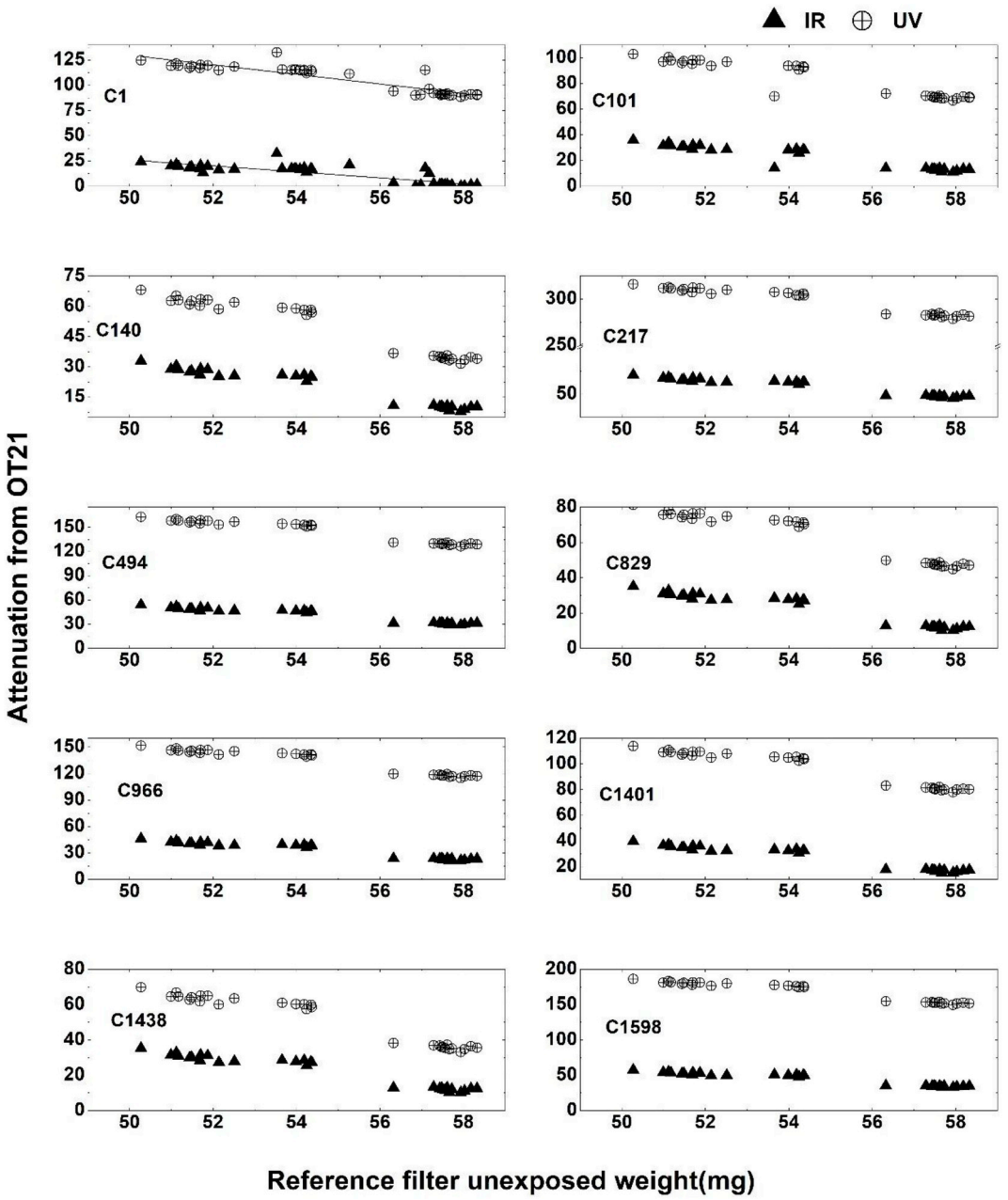

Fig. 3. IR and UV attenuation values for the ten samples against the reference filter unexposed weights. Solid line indicates the linear least square fit.

Transmissometer output, in Fig. 3 the attenuation values obtained for sample filters (shown in Fig. 1) are plotted against the reference filter unexposed weights. The attenuation values indicate approximately a linear pattern with respect to the reference filter unexposed weights: higher attenuation values (for both IR and UV) are observed when the sample filter is measured against a reference filter with lower unexposed weight and vice versa. This result is explained as follows: when the reference filter weighs more than that of the unexposed sample filter, the excess mass in the reference filter results in greater calculated attenuation (see Equation (1)); hence, the instrument output is underestimated. Conversely, a lower-weight reference filter results in the overestimation of the sample filter attenuation. The under and over estimations of the sample filter attenuation is different for IR and UV channels, as is illustrated by the different slopes for IR ($-2.9\,mg^{-1}$) and UV ($-4.7\,mg^{-1}$) for C1 in Fig. 3.

We assumed that Transmissometer output is reliable when the unexposed weights of the sample and reference filter matches, based on Equation (1). We therefore plotted Transmissometer attenuation values for the ten sample filters against the difference in filter weight (sample filter unexposed weight minus reference filter unexposed weight; call this "D"); see Fig. 4. Variations among filters in Fig. 4 are parameterized using linear regression. Solid line in the figure indicates the linear fit. Slope values for IR and UV are

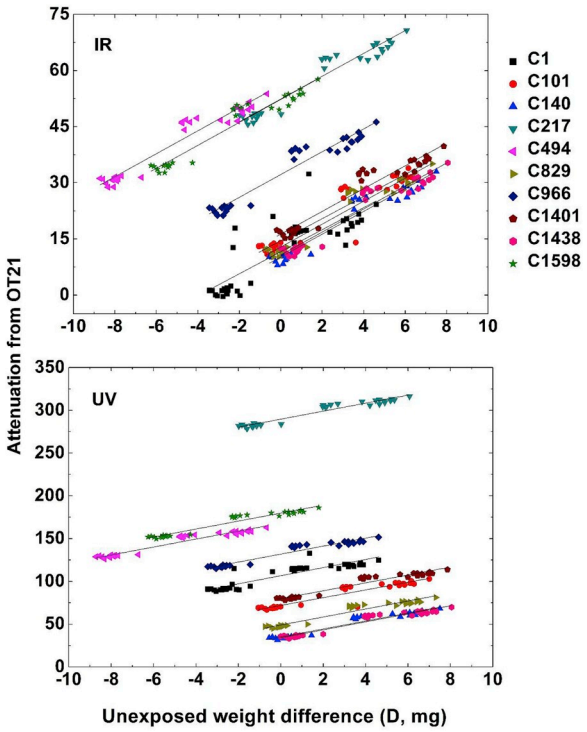

Fig. 4. IR and UV attenuation values against [sample unexposed weight minus reference unexposed weight] for the ten sample filters. Solid and dashed lines indicate best-fit lines.

Table 1
Regression coefficients and 95% Confidence Intervals (CI) for the data shown in Fig. 4.

Filter ID	IR		UV	
	R^2	β_1 (95% CI), mg^{-1}	R^2	β_1 (95% CI), mg^{-1}
C1	0.71	2.9 (2.4–3.5)	0.81	4.7 (4.0–5.4)
C101	0.88	3.0 (2.6–3.3)	0.88	4.5 (3.9–5.1)
C140	0.97	3.0 (2.7–3.3)	0.94	4.7 (4.2–5.1)
C217	0.92	3.1 (2.7–3.4)	0.93	4.6 (4.2–5.1)
C494	0.93	3.1 (2.7–3.4)	0.93	4.7 (4.2–5.1)
C829	0.93	3.1 (2.8–3.4)	0.93	4.7 (4.2–5.1)
C966	0.93	3.0 (2.7–3.4)	0.93	4.7 (4.2–5.1)
C1401	0.92	3.0 (2.7–3.4)	0.93	4.7 (4.2–5.1)
C1438	0.93	3.1 (2.8–3.4)	0.93	4.7 (4.2–5.1)
C1598	0.93	3.1 (2.8–3.4)	0.93	4.7 (4.2–5.1)
All ten filters combined (overall model)	0.90	3.0 (2.7–3.4)	0.94	4.7 (4.2–5.2)

similar across filters (Table 1), suggesting the potential for a correction parameter that could be applied to other filters. In that case, the actual attenuation values of the aerosol sample collected on the sample filter would correspond to a zero value for D.

In addition to the artefact which is identified in the present study, filter-based attenuation measurements are known to suffer from the loading effect, especially when particle loading is high (Park, Hansen, & Cho, 2010; Virkkula et al., 2015). Dutkiewicz et al. (2014) demonstrated the impact of the loading effect on Transmissometer measurements. We observed similar reference filter unexposed weight impact on the sample filter attenuation measurements for a range of loading which gave us confidence that these two effects are independent and need to be corrected separately. The influence of the unexposed weight should be corrected (as it is related to the physical characteristic of the filter paper) before dealing with the loading effect.

4. Correction methodology

Results indicated that for nonzero values of D, Transmissometer output are biased. We considered two correction equations to reduce this bias:

$$Y_i = \beta_o - \beta_1 * D_i + \varepsilon \quad \text{i= 1..N filters} \tag{2}$$

Table 2
IR and UV ATN values corrected using regression equations and matched sample and reference unexposed weights.

Sample ID	Regression (Eq. (2))		Regression (Eq. (3))		Matched unexposed weights	
	Corrected ATN (Y)		Corrected ATN (Y)		Reported ATN (β_o, for D ˜ 0)	
	IR	UV	IR	UV	IR	UV
C1	11.58	105.20	11.58	105.21	–	–
C101	14.74	72.57	14.52	71.94	13.99	70.5
C140	10.29	35.50	10.19	35.02	10.31	33.99
C217	52.38	289.70	52.40	289.67	48.33	283.76
C494	56.15	168.07	56.00	168.08	–	–
C829	11.81	47.74	11.64	47.17	10.20	44.88
C966	32.20	131.86	32.21	131.86	–	–
C1401	16.27	79.53	16.30	79.64	16.93	80.5
C1438	10.93	34.61	10.71	33.95	12.54	35.61
C1598	52.26	179.79	52.19	179.79	49.53	176.38

$$Y_i = \beta_o - \beta_{1,i} * D_i + \varepsilon \quad \text{i= 1..N filters} \tag{3}$$

$$D = (\textit{sample filter unexposed weight} - \textit{reference filter unexposed weight})$$

Y is corrected ATN value accounting for differences in filter weight between the sample and the reference filter; β_o is the uncorrected, instrument-reported attenuation; β_1 is the correction parameter, determined as the slope in Fig. 4, ε is the normally distributed error with a mean value of 0. Equation (2) represents the model with one slope for all filters and equation (3) represents the model where each filter has its own slope. We observed that the model with a single correction parameter (slope) for all filters had a smaller AIC, indicating a better fit to the data. The slopes ($\beta_1 \pm$ standard errors) based on the best fitting model (Equation (2)) were $3.0 \pm 0.2\,mg^{-1}$ for IR, $4.7 \pm 0.3\,mg^{-1}$ for UV (Table 1). The Y values (IR and UV) obtained using Equations (2) and (3) are presented in Table 2.

We compared our results from the regression equations with values from matched unexposed weights of each sample with that of reference filter (from the suite of ~30 filters used), which we assumed to be unbiased. We attempted to identify pairs for which D = 0, though in practice we could only achieve D ˜ 0; here, we implement a requirement that $D < 0.05$ mg. The β_o values for that particular sample and reference filter pair, are also reported in the last column of Table 2. We observed that the ATN values (IR and UV) agree (meaning that the difference in the sample ATN and raw ATN, when D ˜ 0 is less than the instrument's precision) in all the three cases shown in Table 2, implying the proposed regression correction is reliable. For sample filters C1, C494, and C966 we were unable to find a reference filter whose unexposed weight is close to that of sample filter.

To further test the proposed correction, we quantified the uncertainty in the uncorrected and corrected ATN values (for both IR and UV channels) in terms of mean absolute error. The mean absolute difference in the uncorrected ATN and the ATN values for D ˜ 0 (last column of Table 2, which is considered as the best estimate) is employed here as the error in the uncorrected values. The mean absolute difference in the corrected ATN values using overall correction parameter and the ATN values for D ˜ 0 is employed as the error in the corrected values.

The mean absolute error for the IR channel was between 9.2 and 11.9 ATN units among filters (average error: 10.1); applying our correction approach reduced the error to 2.3 ATN units. For the UV channel, the mean absolute error was 12.6–18.3 ATN units (average error: 15.6); applying our correction approach reduced the error to 3.2 ATN units.

Correction parameters (see equation (2)) differ by spectra (IR versus UV) and may differ by filter type (e.g., Emfab vs non-Emfab). Thus, future research could apply the approach developed here to other filter types.

OT21 transmissometer measurements, which involve a sample filter and a reference filter, appear to be biased when those two unexposed filter weights differ. Here, we present evidence of this bias, and then develop and test an approach to correct the bias. For 37 mm Emfab filters, Transmissometer users could adopt the overall correction equation and parameters reported here, which carries the advantage of not requiring new measurements.

5. Summary

The current study brings to light a previously unknown sensitivity in the offline BC measuring instrument, the Sootscan Optical Transmissometer (OT21), in the case of Emfab filters. The findings from the study are summarized as follows:

1. Use of reference filters with higher unexposed weights than that of sample filters resulted in underestimation of the sample attenuation and vice versa.
2. Correction equations and parameters (for UV and IR channels) are proposed (case of Emfab), which allow the user to measure the sample attenuation against any random reference (unexposed) filter, irrespective of batch and lot.
3. The correction methodology proposed in the current study reduced the error in the instrument measured attenuation from 44% (15%) to 10% (3%) for the UV (IR) channel.

Acknowledgements

The research leading to these results received funding from the European Research Council under ERC Grant Agreement number 336167 for the CHAI Project. We are thankful to field staff of CHAI project and Sri Ramachandra University, Chennai for their collaboration throughout the monitoring and measurements. Filter weight data is available from the corresponding author on request.

References

Ahmed, T., Dutkiewicz, V. A., Shareef, A., Tuncel, G., Tuncel, S., & Husain, L. (2009). Measurement of black carbon (BC) by an optical method and a thermal-optical method: Intercomparison for four sites. *Atmospheric Environment, 43*(40), 6305–6311.

Balakrishnan, K., Sambandam, S., Ramaswamy, P., Ghosh, S., Venkatesan, V., Thangavel, G., et al. (2015). Establishing integrated rural–urban cohorts to assess air pollution-related health effects in pregnant women, children and adults in southern India: An overview of objectives, design and methods in the Tamil Nadu air pollution and health effects (TAPHE) study. *BMJ open, 5*(6), e008090.

Baumgartner, J., Zhang, Y., Schauer, J. J., Huang, W., Wang, Y., & Ezzati, M. (2014). Highway proximity and black carbon from cookstoves as a risk factor for higher blood pressure in rural China. *Proceedings of the National Academy of Sciences, 111*(36), 13229–13234.

Bond, T. C., Doherty, S. J., Fahey, D. W., Forster, P. M., Berntsen, T., DeAngelo, B. J., et al. (2013). Bounding the role of black carbon in the climate system: A scientific assessment. *Journal of Geophysical Research: Atmosphere, 118*(11), 5380–5552.

Davy, P. M., Tremper, A. H., Nicolosi, E. M., Quincey, P., & Fuller, G. W. (2017). Estimating particulate black carbon concentrations using two offline light absorption methods applied to four types of filter media. *Atmospheric Environment, 152*, 24–33.

Delumyea, R. G., Lih-Ching, C., & Macias, E. S. (1980). Determination of elemental carbon component of soot in ambient aerosol samples. *Atmospheric Environment, 14*(6), 647–652 1967.

Dutkiewicz, V. A., DeJulio, A. M., Ahmed, T., Laing, J., Hopke, P. K., Skeie, R. B., et al. (2014). Forty-seven years of weekly atmospheric black carbon measurements in the Finnish Arctic: Decrease in black carbon with declining emissions. *Journal of Geophysical Research: Atmosphere, 119*(12), 7667–7683.

Hill, A. S. G. (1936). Measurement of the optical densities of smoke stains on filter papers. *Transactions of the Faraday Society, 32*, 1125–1131.

Janssen, N. A., Hoek, G., Simic-Lawson, M., Fischer, P., Van Bree, L., Ten Brink, H., et al. (2011). Black carbon as an additional indicator of the adverse health effects of airborne particles compared with PM10 and PM2. 5. *Environmental Health Perspectives, 119*(12), 1691.

Kirchstetter, T. W., & Thatcher, T. L. (2012). Contribution of organic carbon to wood smoke particulate matter absorption of solar radiation. *Atmospheric Chemistry and Physics, 12*(14), 6067–6072.

Moosmüller, H., Chakrabarty, R. K., & Arnott, W. P. (2009). Aerosol light absorption and its measurement: A review. *Journal of Quantitative Spectroscopy and Radiative Transfer, 110*(11), 844–878.

Ostro, B. D., Feng, W. Y., Broadwin, R., Malig, B. J., Green, R. S., & Lipsett, M. J. (2008). The impact of components of fine particulate matter on cardiovascular mortality in susceptible subpopulations. *Occupational and Environmental Medicine, 65*(11), 750–756.

Park, S. S., Hansen, A. D., & Cho, S. Y. (2010). Measurement of real time black carbon for investigating spot loading effects of Aethalometer data. *Atmospheric Environment, 44*(11), 1449–1455.

Presler-Jur, P., Doraiswamy, P., Hammond, O., & Rice, J. (2017). An evaluation of mass absorption cross-section for optical carbon analysis on Teflon filter media. *Journal of the Air & Waste Management Association, 67*(11), 1213–1228.

R Core Team (2016). *R: A Language and Environment for Statistical Computing*. https://www.r-project.org/.

Ram, K., Sarin, M. M., & Tripathi, S. N. (2010). Inter-comparison of thermal and optical methods for determination of atmospheric black carbon and attenuation coefficient from an urban location in northern India. *Atmospheric Research, 97*(3), 335–342.

Tonne, C., Salmon, M., Sanchez, M., Sreekanth, V., Bhogadi, S., Sambandam, S., et al. (2017). Integrated assessment of exposure to PM 2.5 in south India and its relation with cardiovascular risk: Design of the CHAI observational cohort study. *International Journal of Hygiene and Environmental Health, 220*(6), 1081–1088.

Virkkula, A., Chi, X., Ding, A., Shen, Y., Nie, W., Qi, X., et al. (2015). On the interpretation of the loading correction of the aethalometer. *Atmospheric Measurement Techniques, 8*(10), 4415–4427.